arXiv:1610.04241v1 [physics.optics] 13 Oct 2016

Envelope time reversal of optical pulses following frequency conversion with accelerating quasi-phase-matching

Michal Yachini, Boris Malomed, and Alon Bahabad

Department of Physical Electronics, School of Electrical Engineering, Fleischman Faculty of Engineering, Tel-Aviv University, Tel-Aviv 69978, Israel

Abstract

It is shown theoretically that the use of accelerating spatiotemporal quasi-phase-matching (QPM) modulation patterns in media with parametric optical interactions makes it possible to generate a time-reversed replica of the pump pulse envelope in a frequency converted signal. The conversion is dependent on the group-velocity mismatch between the fundamental and up-converted harmonics, and controlled by the acceleration rate (*chirp*) of the QPM phase pattern. Analytical results are corroborated by numerical simulations.

Keywords: Time reversal, QPM, chirp, nonlinear

Time reversal of pulses has important applications, such as the correction of wave distortions [1] and focusing in various settings, including complex media, [2] plasmonics, [3] medical ultrasound [4] and communications microwaves. [5] In optics, time reversal was demonstrated or predicted by means of two different methods: by phase conjugation via nonlinear four-wave mixing [6–10] or by using time-modulated photonic structures. [11–17] A recent related result is the inversion of Airy pulses in a linear optical fiber with third-order dispersion. [18] Here we aim to show that the interaction of a pump pulse with an accelerating (chirped) spatiotemporal nonlinear photonic crystal [19,20] can generate a signal pulse which is an envelope-time-reversed, [21] frequency-converted, replica of the pump pulse, provided that group-velocity mismatch is maintained between the pump and signal pulses. Our signal is the result of two actions - envelope time reversal and, considering the bandwidth associated with the signal envelope, broadband frequency conversion. In passing we mention that regardless of time-reversal, there are to date a few known techniques for inducing broadband optical frequency conversion such as autoresonant or adiabatic frequency conversion. [22–26] Our results are also relevant to cases where energy is exchanged between different modes due to a dynamical modulation. [27,28]

Dispersion-induced phase mismatch inhibits efficient optical-frequency conversion processes. To ameliorate the situation in energy-conserving processes, one can use properly patterned spatial modulations of a parameter relevant to the process to compensate for momentum mismatch. This technique is known as Quasi-Phase-Matching (QPM). [29,30] More generally, the phase mismatch may be split between the momentum and energy domains, in which case a spatiotemporal modulation is needed to phase-match the process. Such spatiotemporal QPM was actually demonstrated for high-harmonic-generation, prior to the full theoretical treatment, [19] using a modulation in the form of a constant-velocity grating realized by a train of counter-propagating pulses. [31] The availability of techniques for engineering complex spa-

*To whom correspondence should be addressed

tiotemporal light patterns[32,33] suggests that all-optical spatiotemporal QPM can be produced, using modulations more sophisticated than gratings moving at a constant velocity. In particular, an accelerating grating can enforce different phase-matching (PM) conditions at different times in the course of the nonlinear interaction. Spatiotemporal QPM with specific accelerating modulations were suggested for controlling the temporal and spectral profiles of high-harmonic generation,[20] and for realizing time-to-frequency mapping of optical pulses.[33]

In the following we show that, choosing an accelerating all-optical modulation pattern, one can realize a frequency converted signal having the time-reversed envelope of the optical pump pulse interacting with the pattern. We stress that the method is relevant to any frequency-conversion process in which the group-velocity-mismatch is significant and an all-optical modulation is applicable, both in perturbative[34,35] and in extreme nonlinear optics.[31] Without loss of generality we develop this concept for the prototypical nonlinear frequency conversion of Second-Harmonic-Generation (SHG).

We start with the one-dimensional wave equation for the Second-Harmonic (SH) field in the frequency domain under the no-depletion approximation in a non-magnetic medium:

$$\frac{\partial^2 \tilde{E}_{2\omega_0}(z,\omega)}{\partial z^2}+\beta^2(\omega)\tilde{E}_{2\omega_0}(z,\omega)=-\mu_0\omega^2\tilde{P}_{\mathrm{NL}}(z,\omega), \tag{1}$$

where $n(\omega)$ is the index of refraction, $c=1/\sqrt{\mu_0\varepsilon_0}$ is the speed of light, μ_0 is the vacuum permeability, ε_0 is the vacuum permittivity, and $\beta(\omega)=n(\omega)\omega/c$ is the wavenumber. $\tilde{P}_{\mathrm{NL}}(z,\omega)$ is the Fourier transform of the material second-order nonlinear polarization. In the time domain it is defined as

$$P_{\mathrm{NL}}(z,t)=\varepsilon_0\chi^{(2)}g(z,t)E^2_{\omega_0}(z,t), \tag{2}$$

where $E_{\omega_0}(z,t)$ is the fundamental-harmonic (FH) electric field, $\chi^{(2)}$ is the second-order electric susceptibility, and $g(z,t)=e^{i\Phi(z,t)}$ is the spatiotemporal modulation imposed by the QPM modulation onto the nonlinear polarization. The spatial and temporal frequencies of the phase function $\Phi(z,t)$ can be used to phase match momentum and energy components, respectively.[19]

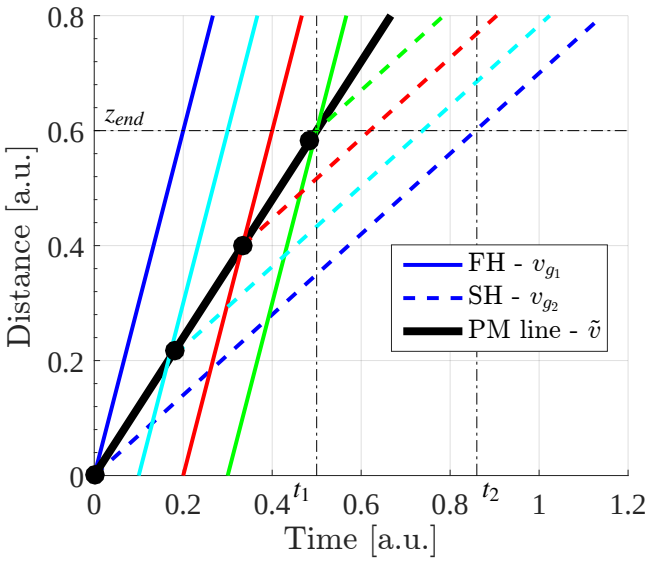

Figure 1: Space-time diagram for envelope time reversal using an accelerating QPM modulation. Along the thick continuous line, corresponding to velocity $\tilde{v}$, the phase-matching (PM) condition is met for SHG. Continuous and dashed lines represent, respectively, wavelets (short segments of the emitted radiation) belonging to the FH pulse and SH radiation propagating at the respective group velocities. Whenever an FH wavelet encounters the PM line, an SH wavelet is emitted. At the end of the interaction, $z=z_{\mathrm{end}}$, the time ordering of the SH wavelets is the time reversal of the FH wavelets.

Our goal is to find a phase-modulation pattern, $\Phi(z,t)$, such that the resulting SH temporal envelope will be the *time reversal* of its squared FH counterpart. First, we assume that, at $z=0$, the FH pulse starts at $t=0$, and the FH (SH) moves at group velocity v_{g_1} (v_{g_2}) with $v_{g_2}<v_{g_1}$. We utilize the difference in group velocities between the SH and the FH as follows: the QPM modulation, as we show below, will satisfy PM conditions only for a short temporal interval around $t=z/\tilde{v}$ (the "PM locus" denoted by the thick continuous line in Fig. 1), where $v_{g_2}<\tilde{v}<v_{g_1}$. In this small temporal interval, efficient up-conversion takes place. Whenever a specific wavelet belonging to the FH pulse moving at velocity v_{g_1} (continuous lines in Fig. 1) hits the PM line, an SH wavelet is emitted, propagating at velocity v_{g_2} (dashed lines in Fig. 1). If the FH pulse width is T_1, the up-conversion pro-

cess will effectively cease at $z_{\text{end}} = v_{g_1}\tilde{v}T_1/(v_{g_1} - \tilde{v})$. Using basic geometrical arguments it is apparent from Fig. 1 that, at this point, the SH envelope is the time reversal of the (squared) FH envelope, scaled with a factor

$$R = \frac{\tilde{v} - v_{g_2}}{v_{g_1} - \tilde{v}} \cdot \frac{v_{g_1}}{v_{g_2}}, \tag{3}$$

such that the SH pulse duration is $T_2 = RT_1$ (note that $t_2 - t_1$ in Fig. 1 is equal to T_2). Note that for $v_{g_2} > v_{g_1}$, the modulation needs to satisfy the condition $v_{g_1} < \tilde{v} < v_{g_2}$ while the PM line is $z = \tilde{v}(t - T_1)$. Now, we proceed to the identification of an appropriate modulation phase function $\Phi(z,t)$ having the following spatial and temporal frequencies:

$$\frac{\partial \Phi}{\partial z} \equiv \Delta k(z,t), \tag{4a}$$

$$\frac{\partial \Phi}{\partial t} \equiv -\Delta\omega(z,t). \tag{4b}$$

Meanwhile, if $\Delta k = 2k(\omega_0) - k(\tilde{\omega})$ and $\Delta\omega = 2\omega_0 - \tilde{\omega}$ are the momentum and energy phase mismatches of the up-conversion process from frequency ω_0 to $\tilde{\omega}$, they must obey the phase-mismatch-compensation condition:[19]

$$\Delta k(z,t) = [\Delta\omega(z,t)n(\tilde{\omega}) + 2\omega_0\{n(\omega_0) - n(\tilde{\omega})\}]/c. \tag{5}$$

As we require Eq. (5) to hold solely along $z = \tilde{v}t$, it is clear that the choice of

$$\Phi(z,t) = \alpha(z - \tilde{v}t)^2 + \Delta k_0 z, \tag{6}$$

with chirp constant (alias acceleration rate) α, satisfies this condition for $\Delta\omega = 0$, provided that Δk_0 is the momentum mismatch in the case of zero energy mismatch: $\Delta k_0 = 2\omega_0[n(\omega_0) - n(2\omega_0)]/c$. In this case, the PM condition brings the upconversion exactly to the second harmonic, $2\omega_0$.

Of course, this modulation format is not the only one possible for our purpose, but it is, arguably, the simplest one. The temporal acceleration rate of the modulation (chirp) is $\partial^2\Phi/\partial t^2 = 2\alpha\tilde{v}^2$. Faster acceleration moves points outside the PM line farther from the PM conditions, making the accuracy of the envelope time reversal better. To support a required temporal resolution ΔT associated with bandwidth $\Delta\Omega_p = 2\pi/\Delta T$, the QPM-modulation bandwidth in this interval, $\Delta\Omega_m = 2\alpha\tilde{v}^2\Delta T$, must be much larger: $\Delta\Omega_m \gg \Delta\Omega_p$. This resolution condition may be quantified by a figure of merit, F:

$$F = \frac{\Delta\Omega_m}{\Delta\Omega_p} = \alpha\tilde{v}^2\Delta T^2/\pi >> 1 \tag{7}$$

Since $\tilde{v}$ is restricted by the material group velocities, for the required resolution Eq. (7) imposes an essential condition on the chirp constant α of the QPM modulation.

Apart from the desired phase-matched envelope time-reversal process, the proposed modulation format may support other phase-matched upconversion processes. This can be seen as Eqs. (4), (5), and (6) lead to the following condition:

$$2\omega_0\left[\frac{1}{\tilde{v}} - \frac{n(2\omega_0)}{c}\right] = \tilde{\omega}\left[\frac{1}{\tilde{v}} - \frac{n(\tilde{\omega})}{c}\right]. \tag{8}$$

It is evident that the desired upconversion to $\tilde{\omega} = 2\omega_0$ meets this criteria as planned. However, it is possible that the conversion to other frequencies will satisfy this condition as well, depending on the material dispersion and on the chosen velocity, $\tilde{v}$. Such concomitant phase-matched processes will produce additional replicas of the FH around different central frequencies. As long as these replicas stay well separated in the frequency domain, the desired envelope-time-reversed signal can be filtered out. The time orientation of any replica with respect to the FH depends on the replica's group velocity $v_{g_{\tilde{\omega}}}$ (and its relation to the FH group velocity and the spatiotemporal trajectory determined by the PM condition).

A simple analytical model can explicitly demonstrate that the modulation format proposed here indeed results in envelope time reversal. To this end, we use the spatiotemporal slowly-varying-envelope approximation, along with no-depletion approximation for the FH field. Also neglecting higher-order dispersion, we reduce Eq. (1) to:

$$\left(\frac{\partial}{\partial z} + \frac{1}{v_{g_2}}\frac{\partial}{\partial t}\right)A_2(z,t) = \kappa e^{i\Phi(z,t)}A_1^2\left(t - \frac{z}{v_{g_1}}\right), \tag{9}$$

where A_1 (A_2) is the FH (SH) envelope, $\kappa \equiv$

$-i\omega_{SH}^2 d_{\rm eff}/[c^2 k(\omega_{\rm SH})]$ and $d_{\rm eff}$ is the nonlinear-coupling coefficient. We make use of a coordinate system moving with the SH group velocity, so that $\tau_2 = t - z/v_{g_2}$, $\xi = z$. In this case, Eq. (9) becomes:

$$\frac{\partial}{\partial \xi} A_2(\xi,\tau_2) = \kappa e^{i\Phi(\xi,\tau_2)} A_1^2 \left[\tau_2 + \xi\left(\frac{1}{v_{g_2}} - \frac{1}{v_{g_1}}\right)\right]. \tag{10}$$

Assuming that the acceleration of the QPM modulation pattern is large enough, we use the stationary-phase approximation to integrate Eq. (10) around the stationary points ξ_s determined by $\partial\Phi/\partial\xi|_{\xi_s} = 0$, which yields

$$\xi_s = \frac{\Delta k_0}{2\alpha(1-\tilde{v}/v_{g_2})^2} + \frac{\tilde{v}\tau_2}{1-\tilde{v}/v_{g_2}} \approx \frac{\tilde{v}\tau_2}{1-\tilde{v}/v_{g_2}} \tag{11}$$

under the above condition, $\alpha \gg \Delta k_0$ (the stationary point-equation is tantamount to the definition of the PM line, $z = \tilde{v}t$). Integration gives

$$\begin{aligned} A_2(\xi,\tau_2) &\approx A_1^2\left(\tau_2 + \xi_s\left(\frac{1}{v_{g2}} - \frac{1}{v_{g1}}\right)\right) e^{-i\Phi(\xi_s,\tau_2)} \kappa \\ &\times \int_0^\infty \exp\left[-\frac{i\Phi''(\xi_s,\tau_2)}{2}(\xi-\xi_s)^2\right] d\xi = \\ &= \frac{\kappa}{2}\sqrt{\frac{2\pi}{|\Phi''(\xi_s,\tau_2)|}} e^{\pi i/4} \exp\left[i\Phi(\xi_s,\tau_2)\right] \\ &\times A_1^2\left(\tau_2 + \xi_s\left(\frac{1}{v_{g2}} - \frac{1}{v_{g1}}\right)\right). \end{aligned} \tag{12}$$

Substituting ξ_s and getting back to the (z,t) coordinate system, we obtain:

$$\begin{aligned} &A_2(z,t) = \\ &= \kappa\sqrt{\frac{\pi}{|\alpha|(1-\tilde{v}/v_{g_2})^2}} e^{\pi i/4} \exp\left[i\Delta k_0 \frac{\tilde{v}(v_{g_2}t - z)}{v_{g_2} - \tilde{v}}\right] \\ &= A_1^2\left(-\frac{1}{R}\left(t - \frac{z}{v_{g_2}}\right)\right), \end{aligned} \tag{13}$$

where the factor R, given by Eq. (3), is positive for $v_{g_2} < \tilde{v} < v_{g_1}$, which secures the envelope time reversal. Having this result, a few remarks are in order. Essentially we are interested in time reversal as concerns the absolute square of the field, which is accomplished here. The absolute value of the envelope of the SH is not specially sensitive to possible sign changes in the FH (zero crossings). As concerns the phase profile of the SH envelope, it is twice the time-reversed phase of the FH envelope, with an added linear term. We also note that chirp added to the FH field will modify the actual PM condition, which will then deviate from a straight line in space-time, resulting in some distortion in the envelope-time-reversed wave form. Still, for large enough constant α of the accelerating modulation (which represents the intrinsic chirp of the transformation) such distortions will be negligible. Finally, we observe that the SH amplitude scales as $1/|\alpha|$, hence better resolution due to larger α comes at the price of a lower amplitude of the generated SH.

To demonstrate envelope time reversal using our proposed accelerating modulation format, we have performed direct numerical integration of the full wave equation (1), using the procedure outlined in Ref.[33] As an input, we took an FH pulse with central wavelength at 800 nm, propagating in Barium borate (BBO).[36] The modulation format is introduced with the help of the phase function Φ in Eq. (2), while in other settings the amplitude modulation of the nonlinear polarization may also be used.[34,35]

First we look at the FH pulse of an overall duration ~ 1 ps with an asymmetric envelope containing three peaks, distanced 0.3 ps apart, with increasing amplitudes, see Fig. 2(a). The results are displayed in the reference frame moving at the FH group velocity, so that $\tau = t - z/v_{g_1}$, $\xi = z$. The group velocities are $v_{g_1} = 1.78\cdot 10^8$ m/s and $v_{g_2} = 1.68\cdot 10^8$ m/s. The value of $\tilde{v} = 1.76\cdot 10^8$ m/s, substituted in Eq. (3), yields the scaling factor $R \approx 4$. We used four accelerating QPM modulation formats with increasing values of the chirp rate α, so that the corresponding resolution figure of merit F, defined in Eq. (7), increases from 1 to 50, keeping the target resolution of $\Delta T = 0.3$ ps. The respective shapes of the SH envelope produced by the interaction are displayed in Fig. 2(b-e). It is evident that a large enough factor, $F = 50$, secures obtaining an exact envelope-time-reversed replica of the squared FH envelope. To estimate typical parameters, we notice that, in the case of the FH pulse of duration ~ 1 ps, with $\Delta T = 0.3$ ps and $F = 10$, for which the envelope-time-reversed replica has decent resolution, the overall band-

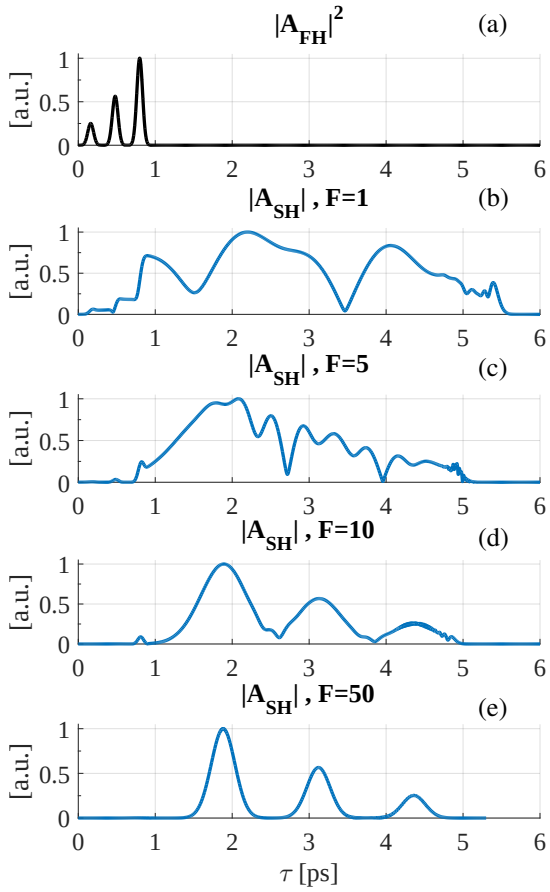

Figure 2: Envelope time reversal for varying acceleration rates of the QPM modulation. (a) The squared absolute value of the field in the FH pulse at the start of the interaction. (b)-(e) The absolute value of the SH field after completing the interaction with the accelerating QPM modulation structure. The results are characterized by values of the resolution-figure-of-merit, F, at different acceleration rates.

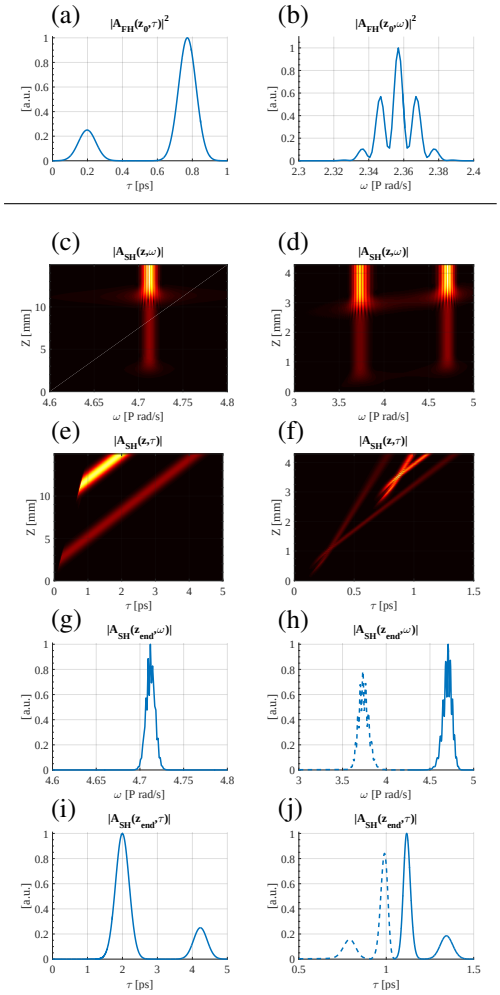

Figure 3: Full temporal and spectral evolution of radiation emitted due to the interaction of an FH with the accelerating QPM modulation. Top panel: (a) temporal and (b) spectral dependence of the FH field. Bottom panel: left column: evolution of the SH for a QPM modulation allowing for a single envelope-time-reversed SH replica of the FH; right column: evolution of the up-converted radiation for the case of a QPM modulation allowing for an additional non-reversed replica of the FH. (c),(d) spectral evolution (e),(f) temporal evolution (g),(h) the up-converted spectrum at the end of the interaction (i),(j) the up-converted amplitude in the time domain at the end of the interaction. (The non-reversed replica is marked with a dashed line)

width of the QPM modulation is 210 nm for the central wavelength of 800 nm. Such bandwidths are readily achievable with commercial femtosecond lasers.

Next we will look at the full temporal and spectral evolution of the SH field along the interaction coordinate for two different velocities, $\tilde{v} = 1.76 \cdot 10^8$ and $1.71 \cdot 10^8$ m/s, while $\alpha = 5 \cdot 10^{10}$ rad/m^2 for both cases. Together with the target value of $\Delta T = 0.55$ ps, one has the corresponding values $F = 150$ and 140 for the two cases. This time, the FH field has an asymmetric double-peak envelope with a 1 ps duration, see Fig. 3(a). For $\tilde{v} = 1.76 \cdot 10^8$ m/s the QPM modulation gives rise precisely to the intended envelope-time-reversed shape of the SH, as seen in Fig. 3(i). In this case, the temporal evolution clearly shows that the two peaks of the FH profile are generated at different coordinates. Although the earlier FH peak is upconverted first, at the end of the interaction it lags behind the upconverted second peak, because

the SH group velocity is smaller than both the FH group velocity and the velocity $\tilde{v}$ selected by the PM condition (5). Thus, the sequence of the two peaks in the SH envelope is reversed versus the original FH envelope.

For the second case, with $\tilde{v} = 1.71 \cdot 10^8$ m/s, the modulation supports the envelope-time-reversed replica at $\tilde{\omega} = 2\omega_0$, shown by a continuous line in Fig. 3(j), and an additional spectrally separated, non-reversed replica, shown by a dashed line in Fig. 3(j), at $\tilde{\omega} = 1.6\omega_0$, in accordance with Eq. (8). The second replica is not inverted because its group velocity, $1.735 \cdot 10^8$ m/s, is higher than the PM condition velocity $\tilde{v}$ although the order of generation of the two peaks in the SH is the same as in the inverted replica. We note that the QPM modulations are different for the two cases, as they depend on the value of $\tilde{v}$, leading also to a difference in the scaling factors: $R \approx 4\,(0.4)$ for $\tilde{v} = 1.76 \cdot 10^8\,(1.71 \cdot 10^8)$ m/s.

As noted above, our model neglects high-order dispersion terms. This means that for a reliable envelope-time-reversal the interaction length should be shorter than the dispersion length $l_D \equiv T_1^2/\beta_2$ (T_1 is the FH pulse duration and β_2 is its group velocity dispersion) at which dispersion starts to significantly distorts the pump pulse. In typical situations such as considered here (i.e. picosecond duration pump pulse propagating in BBO), this is far from being an actual limitation as the interaction length is about a centimeter while the dispersion length is several meters.

To conclude, we have shown that accelerating (chirped) spatiotemporal quasi-phase-matching modulation can be used for up-converting an FH field to an envelope-time-reversed replica under the non-depletion approximation and when higher-order dispersion is negligible. The choice of the appropriate QPM modulation is dependent on the group-velocity mismatch between the interacting fields. Similarly to other proposed methods of time reversal,[6–8,11–13] the proposed modulation needs to be synchronized with the time of arrival of the FH field, and its bandwidth must be much larger than the bandwidth of the FH, to secure high-quality inversion. The latter condition is controlled by the chirp rate of the QPM modulation. While we have demonstrated the proposed scheme in detail using the most fundamental nonlinear process of SHG, it should be relevant to any nonlinear optical process based on parametric interactions, such as high-harmonic generation, where the nonlinear polarization can be manipulated macroscopically using an all-optical perturbation with high efficiency.[31] Finally, we note that the use of all-optical accelerating modulations that we discussed here might also find use in other scenarios including chromatic dispersion compensation,[8,37] and solitons manipulation.[38]

M.Y and A.B acknowledge support from the Israel Science Foundation (ISF) (1233/13). The work of B.A.M. is supported, in part, by grant No. 2015616 from the joint program in physics between NSF and Binational (US-Israel) Science Foundation.

References

(1) Agarwal, G.; Friberg, A. T.; Wolf, E. Scattering theory of distortion correction by phase conjugation. *J. Opt. Soc. Am.* **1983**, *73*, 529–538.

(2) Aulbach, J.; Gjonaj, B.; Johnson, P. M.; Mosk, A. P.; Lagendijk, A. Control of light transmission through opaque scattering media in space and time. *Phys. Rev. Lett.* **2011**, *106*, 103901.

(3) Li, X.; Stockman, M. I. Highly efficient spatiotemporal coherent control in nanoplasmonics on a nanometer-femtosecond scale by time reversal. *Phys. Rev. B* **2008**, *77*, 195109.

(4) Fink, M. Time-reversal mirrors. *J. Phys. D: Appl. Phys.* **1993**, *26*, 1333.

(5) Lerosey, G.; De Rosny, J.; Tourin, A.; Fink, M. Focusing beyond the diffraction limit with far-field time reversal. *Science* **2007**, *315*, 1120–1122.

(6) Yariv, A.; Fekete, D.; Pepper, D. M. Compensation for channel dispersion by nonlinear optical phase conjugation. *Opt. Lett.* **1979**, *4*, 52–54.

(7) Miller, D. Time reversal of optical pulses by four-wave mixing. *Opt. Lett.* **1980**, *5*, 300–302.

(8) Kuzucu, O.; Okawachi, Y.; Salem, R.; Foster, M. A.; Turner-Foster, A. C.; Lipson, M.; Gaeta, A. L. Spectral phase conjugation via temporal imaging. *Opt. Express* **2009**, *17*, 20605–20614.

(9) Marom, D.; Panasenko, D.; Rokitski, R.; Sun, P.-C.; Fainman, Y. Time reversal of ultrafast waveforms by wave mixing of spectrally decomposed waves. *Opt. Lett.* **2000**, *25*, 132–134.

(10) Joubert, C.; Roblin, M. L.; Grousson, R. Temporal reversal of picosecond optical pulses by holographic phase conjugation. *Appl. Opt.* **1989**, *28*, 4604–4612.

(11) Yanik, M. F.; Fan, S. Time reversal of light with linear optics and modulators. *Phys. Rev. Lett.* **2004**, *93*, 173903.

(12) Longhi, S. Stopping and time reversal of light in dynamic photonic structures via Bloch oscillations. *Phys. Rev. E* **2007**, *75*, 026606.

(13) Sivan, Y.; Pendry, J. B. Time reversal in dynamically tuned zero-gap periodic systems. *Phys. Rev. Lett.* **2011**, *106*, 193902.

(14) Sanghoon, C.; Primerov, N.; Song, K. Y.; Thévenaz, L.; Santagiustina, M.; Ursini, L. True time reversal via dynamic Brillouin gratings in polarization maintaining fibers. Nonlinear Photonics. 2010; p NThA6.

(15) Zheng, Y.; Ren, H.; Wan, W.; Chen, X. Time-reversed wave mixing in nonlinear optics. *Sci. Rep.* **2013**, *3*.

(16) Chumak, A. V.; Tiberkevich, V. S.; Karenowska, A. D.; Serga, A. A.; Gregg, J. F.; Slavin, A. N.; Hillebrands, B. All-linear time reversal by a dynamic artificial crystal. *Nat. Commun.* **2010**, *1*, 141.

(17) Yanik, M. F.; Fan, S. Dynamic photonic structures: stopping, storage, and time reversal of light. *Stud. Appl. Math.* **2005**, *115*, 233–253.

(18) Driben, R.; Hu, Y.; Chen, Z.; Malomed, B. A.; Morandotti, R. Inversion and tight focusing of Airy pulses under the action of third-order dispersion. *Opt. Lett.* **2012**, *38*, 2499–2501.

(19) Bahabad, A.; Murnane, M. M.; Kapteyn, H. C. Quasi-phase-matching of momentum and energy in nonlinear optical processes. *Nat. Photonics* **2010**, *4*, 570–575.

(20) Bahabad, A.; Murnane, M. M.; Kapteyn, H. C. Manipulating nonlinear optical processes with accelerating light beams. *Phys. Rev. A* **2011**, *84*, 033819.

(21) Sivan, Y.; Pendry, J. B. Theory of wavefront reversal of short pulses in dynamically tuned zero-gap periodic systems. *Phys. Rev. A* **2011**, *84*, 033822.

(22) Yaakobi, O.; Friedland, L. Autoresonant four-wave mixing in optical fibers. *Phys. Rev. A* **2010**, *82*, 023820.

(23) Yaakobi, O.; Clerici, M.; Caspani, L.; Vidal, F.; Morandotti, R. Complete pump depletion by autoresonant second harmonic generation in a nonuniform medium. *J. Opt. Soc. Am. B* **2013**, *30*, 1637–1642.

(24) Suchowski, H.; Porat, G.; Arie, A. Adiabatic processes in frequency conversion. *Laser Photonics Rev.* **2014**, *8*, 333–367.

(25) Moses, J.; Suchowski, H.; Kärtner, F. X. Fully efficient adiabatic frequency conversion of broadband Ti: sapphire oscillator pulses. *Opt. Lett.* **2012**, *37*, 1589–1591.

(26) Rangelov, A. A.; Vitanov, N. V. Broadband sum-frequency generation using cascaded processes via chirped quasi-phase-matching. *Phys. Rev. A* **2012**, *85*, 045804.

(27) Karenowska, A. D.; Gregg, J.; Tiberkevich, V.; Slavin, A.; Chumak, A.; Serga, A.; Hillebrands, B. Oscillatory energy exchange between waves coupled by a dynamic artificial crystal. *Phys. Rev. Lett.* **2012**, *108*, 015505.

(28) Sivan, Y.; Rozenberg, S.; Halstuch, A.; Ishaaya, A. Nonlinear wave interactions between short pulses of different spatio-temporal extents. *Sci. Rep.* **2016**, *6*.

(29) Boyd, R. W. *Nonlinear optics*; Academic press, 2003.

(30) Armstrong, J.; Bloembergen, N.; Ducuing, J.; Pershan, P. Interactions between light waves in a nonlinear dielectric. *Phys. Rev* **1962**, *127*, 1918.

(31) Zhang, X.; Lytle, A. L.; Popmintchev, T.; Zhou, X.; Kapteyn, H. C.; Murnane, M. M.; Cohen, O. Quasi-phase-matching and quantum-path control of high-harmonic generation using counterpropagating light. *Nat. Phys.* **2007**, *3*, 270–275.

(32) Akturk, S.; Gu, X.; Bowlan, P.; Trebino, R. Spatio-temporal couplings in ultrashort laser pulses. *J. Opt.* **2010**, *12*, 093001.

(33) Konsens, M.; Bahabad, A. Time-to-frequency mapping of optical pulses using accelerating quasi-phase-matching. *Phys. Rev. A* **2016**, *93*, 023823.

(34) Bahabad, A.; Cohen, O.; Murnane, M. M.; Kapteyn, H. C. Quasi-phase-matching and dispersion characterization of harmonic generation in the perturbative regime using counterpropagating beams. *Opt. Express* **2008**, *16*, 15923–15931.

(35) Myer, R.; Penfield, A.; Gagnon, E.; Lytle, A. L. Enhancing the Conversion Efficiency of Second Harmonic Generation Using Counterpropagating Light. Front. Opt. 2014. 2014; p FTh4C.4.

(36) Eimerl, D.; Davis, L.; Velsko, S.; Graham, E.; Zalkin, A. Optical, mechanical, and thermal properties of barium borate. *J. Appl. Phys.* **1987**, *62*, 1968–1983.

(37) Watanabe, S.; Naito, T.; Chikama, T. Compensation of chromatic dispersion in a single-mode fiber by optical-phase conjugation. *IEEE Photonics Technol. Lett.* **1993**, *5*, 92–96.

(38) Afanasjev, V. V.; Malomed, B. A.; Chu, P. L. Dark soliton generation in a fused coupler. *Opt. Commun.* **1997**, *137*, 229–232.